

## The Luminescence of $\text{Cs}_3\text{Bi}_2\text{Cl}_9$ and $\text{Cs}_3\text{Sb}_2\text{Cl}_9$

C. W. M. TIMMERMANS, S. O. CHOLAKH,\* AND G. BLASSE

*Physical Laboratory, State University, P.O. Box 80.000, 3508 TA Utrecht, The Netherlands*

Received July 22, 1982

The luminescence properties of  $\text{Cs}_3\text{Bi}_2\text{Cl}_9$ ,  $\alpha\text{-Cs}_3\text{Sb}_2\text{Cl}_9$ , and  $\beta\text{-Cs}_3\text{Sb}_2\text{Cl}_9$  are reported and compared with those of  $\text{Cs}_3\text{Bi}_2\text{Br}_9$ . The first two compounds have comparable luminescence properties which can be described in terms of a band model. Deep center emission is observed for both compounds, whereas edge emission is observed only for  $\text{Cs}_3\text{Bi}_2\text{Cl}_9$ . The optical transitions of  $\beta\text{-Cs}_3\text{Sb}_2\text{Cl}_9$  are localized on the  $\text{Sb}^{3+}$  ion. The orientation of the lone-pair orbitals of the  $ns^2$  ions seems to play an important role in the formation of the cationic valence band. The  $\alpha\text{-}\beta$  transformation must therefore have a considerable influence on the spectral properties of  $\text{Cs}_3\text{Sb}_2\text{Cl}_9$ .

### Introduction

In a previous paper we reported on the luminescence of  $\text{Cs}_3\text{Bi}_2\text{Br}_9$  (1). In that paper it was shown that the optical properties of this compound must be described in terms of a band model analogous to the cesium lead halides (2, 3), with which  $\text{Cs}_3\text{Bi}_2\text{Br}_9$  is, in first approximation, isostructural and isoelectrical. Band structure calculations for  $\text{CsPbCl}_3$  and  $\text{CsPbBr}_3$  show that the top of the valence band consists of the cationic  $6s$  functions and the  $p$  functions of the anions (3). The bottom of the conduction band is formed by the cationic  $6p$  functions. The band gap transition is intracationic.

In the excitation spectrum of  $\text{Cs}_3\text{Bi}_2\text{Br}_9$  we observed a sharp excitonic transition at about 6 meV below the band edge which is at 2.7 eV. At higher energies a broad excitation band was found which was ascribed to

a charge transfer transition from the bromine  $4p$  band to the bismuth conduction band. In emission free-exciton recombination was observed in addition to the luminescence of several impurity centers (1, 4).

It seemed interesting to investigate the compounds  $\text{Cs}_3\text{Bi}_2\text{Cl}_9$  and  $\alpha\text{-}$  and  $\beta\text{-Cs}_3\text{Sb}_2\text{Cl}_9$  in view of the correspondence in crystal structure between these compounds and  $\text{Cs}_3\text{Bi}_2\text{Br}_9$ . Since the cationic orbitals in these compounds are on the boundary between being localized and delocalized (1), unexpected results cannot be ruled out.

The compound  $\text{Cs}_3\text{Bi}_2\text{Cl}_9$  shows two different configurations (5). At high temperatures it has a structure which is essentially the same as the structure of  $\text{Cs}_3\text{Bi}_2\text{Br}_9$  (6). This structure consists of a cubic close-packing of  $\text{CsCl}_3$  layers (ABCABC) in which two-thirds of the interstitial octahedral chlorine holes are occupied by  $\text{Bi}^{3+}$  ions in such a way that double layers of bismuth and chlorine are formed. At 373°C

\* On leave from Urals Polytechnical Institute, P.B. 620002, Sverdlovsk, U.S.S.R.

a phase transition occurs. Below this temperature the  $\text{CsCl}_3$  layers are packed with layer sequence ABACBC (7). The bismuth ions then form double chains parallel to the  $a$  axis. There are two different sites for the bismuth ions.

The compound  $\text{Cs}_3\text{Sb}_2\text{Cl}_9$  can be obtained from an aqueous solution in two different forms: the  $\alpha$  form, which has the same structure as the high-temperature modification of  $\text{Cs}_3\text{Bi}_2\text{Cl}_9$  (8), and the  $\beta$  form, which is isostructural with the low-temperature modification of  $\text{Cs}_3\text{Bi}_2\text{Cl}_9$  (7).

The trivalent metal ions in these compounds have  $s^2$  configuration. They have a tendency to form  $\text{MeX}_3$  molecules (i.e., three short and three longer metal-halide distances). This is due to the  $s^2$  lone pair of such ions which points away from the short metal-halide bonds.

The crystallographic data for the above-mentioned compounds are listed in Table I.

## Experimental

Single crystals of  $\text{Cs}_3\text{Bi}_2\text{Cl}_9$  and  $\text{Cs}_3\text{Sb}_2\text{Cl}_9$  were grown by dissolving stoichiometric amounts of  $\text{CsCl}$  and the metal sesquioxides in a concentrated  $\text{HCl}$  solution followed by slow evaporation of the saturated solution.  $\text{Cs}_3\text{Bi}_2\text{Cl}_9$  crystals were colorless. They showed an absorption edge near 3.14 eV at 80K. Crystals of  $\alpha$ - and  $\beta$ - $\text{Cs}_3\text{Bi}_2\text{Cl}_9$  were grown from the same solution. After crystallization they were selected under a microscope. The  $\alpha$ - $\text{Cs}_3\text{Sb}_2\text{Cl}_9$  crystals were hexagonal plates with a brownish color. The absorption edge of these crystals was at about 3.0 eV at room temperature. Crystals of  $\beta$ - $\text{Cs}_3\text{Sb}_2\text{Cl}_9$  were pale-yellow rods, but we were also able to grow colorless crystals of this compound from the remaining mother liquor.

The apparatus used for recording the emission and excitation spectra and measuring the decay times has been described in (1). Decay times of the cesium antimony

chlorides were partially measured on an apparatus described in (9).

## Results and Discussion

### 1. Luminescence of $\text{Cs}_3\text{Bi}_2\text{Cl}_9$

At liquid helium temperature the absorption spectrum of a  $\text{Cs}_3\text{Bi}_2\text{Cl}_9$  crystal starts with a sharp line at 3.140 eV followed by some weaker lines at 3.142, 3.145, and 3.152 eV (see Fig. 1). Above 3.16 eV the absorption rises steeply. The  $\text{Cs}_3\text{Bi}_2\text{Cl}_9$  crystals show luminescence at low temperatures only. The emission is situated in the red part of the spectrum. This is in contrast with  $\text{Cs}_3\text{Bi}_2\text{Br}_9$ , which shows at 4.2K bright edge luminescence next to red luminescence (1). In Fig. 2 we give the emission and excitation spectra of the luminescence of  $\text{Cs}_3\text{Bi}_2\text{Cl}_9$  at liquid helium temperature. In the band edge region the excitation spectrum corresponds to the absorption spectrum: at 3.140 eV a sharp line is followed by a narrow band with a maximum at 3.20 eV

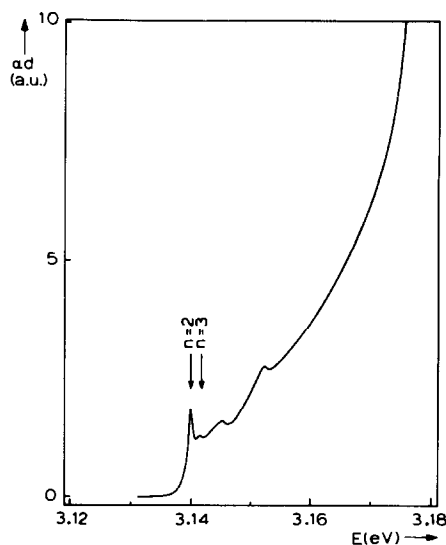


FIG. 1. Absorption spectrum of a  $\text{Cs}_3\text{Bi}_2\text{Cl}_9$  single crystal at 4.2K. The optical density is given in arbitrary units. Exciton absorptions indicated by arrows form a Wannier series from which the  $n = 1$  exciton is absent (see text).

TABLE I  
CRYSTALLOGRAPHIC DATA FOR THE CESIUM BISMUTH HALIDES AND THE CESIUM ANTIMONY CHLORIDES

	Cs <sub>3</sub> Bi <sub>2</sub> Br <sub>9</sub> (6)	Cs <sub>3</sub> Bi <sub>2</sub> Cl <sub>9</sub> (h.t.) (5)	Cs <sub>3</sub> Bi <sub>2</sub> Cl <sub>9</sub> (l.t.) (7)	α-Cs <sub>3</sub> Sb <sub>2</sub> Cl <sub>9</sub> (8)	β-Cs <sub>3</sub> Sb <sub>2</sub> Cl <sub>9</sub> (7)
Unit cell (Å)	<i>a</i> = 7.972	<i>a</i> = 7.658 <sup>a</sup>	<i>a</i> = 7.644 <i>b</i> = 13.227 <i>c</i> = 18.684	<i>a</i> = 7.633 <i>c</i> = 9.345	<i>a</i> = 7.630 <i>b</i> = 13.079 <i>c</i> = 18.663
<i>Z</i>	1	1	4	1	4
Space group	<i>P3m1</i>	<i>P321</i>	<i>Pmcn</i>	<i>P321</i>	<i>Pmcn</i>
Metal-halogen distances (Å)	2.71 (3×) 2.98 (3×)	2.48 (3×) 2.90 (3×)	Bi(1)2.48 (2×) 2.55 (1×) 2.60 (1×) 2.84 (2×) Bi(2)2.47 (1×) 2.56 (2×) 2.83 (2×) 3.08 (1×)	2.42 (3×) 2.82 (3×)	Sb(1)2.42 (2×) 2.45 (1×) 2.89 (2×) 2.90 (1×) Sb(2)2.52 (2×) 2.53 (1×) 2.81 (2×) 2.81 (1×)

<sup>a</sup> Lattice constants are calculated for room temperature.

(see Fig. 2). The excitation spectrum shows two further broad bands at about 3.4 and 3.8 eV. The relative intensity of the former depends on the emission wavelength monitored, and that of the latter does not.

In emission two broad bands were found, viz., at 1.5 and at 1.9 eV. The former could

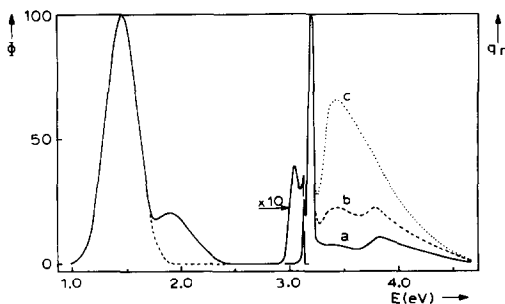


FIG. 2. Emission and excitation spectra of the luminescence of Cs<sub>3</sub>Bi<sub>2</sub>Cl<sub>9</sub> at 4.2K. The emission spectra were recorded for excitation into the band edge at 3.2 eV (solid line) and at 3.4 eV (broken line). Excitation spectra were recorded for emission energies of (a) 2.0 eV, (b) 1.8 eV, and (c) 1.6 eV. Here and in other figures  $\phi$  denotes the photon flux per constant energy interval in arbitrary units and  $q_r$  the relative quantum output.

be excited preferentially in the 3.4-eV excitation band, the latter in the band edge region (see Fig. 2). Upon excitation at 3.20 eV very weak edge luminescence was observed as well. It consists of a sharp line at 3.132 eV followed on the low-energy side by a narrow emission band peaking at 3.05 eV. The experimental accuracy is such that we must conclude that the sharp line in emission does not coincide with the one in the excitation and absorption spectrum.

Figure 3 gives the temperature dependence of the decay time and of the emission intensity of the 1.5-eV emission band. The emission intensity is within the experimental error constant up to about 40K, where thermal quenching occurs. The activation energy for quenching is 54 meV. The decay time vs temperature curve shows below 3K a moderately long decay time of about 80  $\mu$ sec. Above this temperature the decay time decreases to a level of 35–25  $\mu$ sec between 15 and 50K. Above 50K the decay time decreases further due to thermal quenching of the luminescence. All decay curves were single exponentials. The acti-

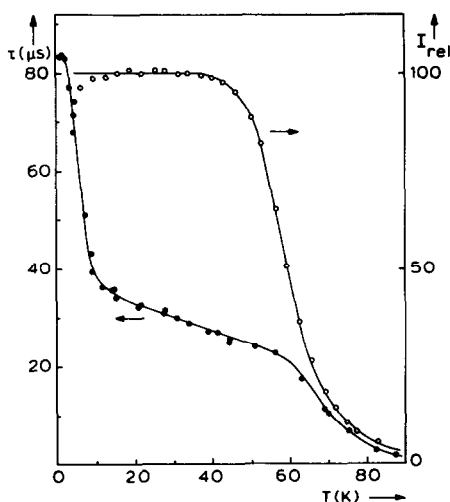


Fig. 3. Emission intensity (O) and decay time (●) of the 1.5-eV emission band of Cs<sub>3</sub>Bi<sub>2</sub>Cl<sub>9</sub> as a function of temperature. The excitation energy was 3.67 eV (N<sub>2</sub>-laser line).

vation energy for the first decrease was about 1 meV and probably corresponded to the energy difference between the <sup>3</sup>P<sub>0</sub> and <sup>3</sup>P<sub>1</sub> levels of an isolated Bi<sup>3+</sup> center (10). We were not able to measure with sufficient accuracy the decay time vs temperature curve of the 1.9-eV emission. The quenching temperature of this emission band is about 50K.

The excitation spectrum of Cs<sub>3</sub>Bi<sub>2</sub>Cl<sub>9</sub> may be interpreted in the same way as we did for Cs<sub>3</sub>Bi<sub>2</sub>Br<sub>9</sub>. The strong narrow band at 3.20 eV corresponds to the band gap transition. The sharp line at 3.140 eV is a cationic exciton transition. The transition is probably a direct one in view of the small half-width of this line (~1 meV). If the transition to the conduction band were indirect, the exciton line would be much broader, if present at all. The low intensity of this transition in the absorption spectrum also makes it improbable that the transition is a direct allowed one.

Elliott deduced expressions for the absorption coefficient of semiconductors in the presence of exciton effects (11). For a

direct allowed transition he gave the absorption coefficient as

$$\alpha = A\gamma e^{\pi\gamma} E^{1/2} / \sinh(\pi\gamma)$$

and for a direct forbidden one as

$$\alpha = A\gamma(1 + \gamma^2)e^{\pi\gamma} E^{3/2} / \sinh(\pi\gamma).$$

In these expressions  $E = h\nu - E_g$  and  $\gamma = (G/E)^{1/2}$ ;  $G$  is the binding energy of the exciton, and  $E_g$  the band gap energy. When  $E \gg G$ ,  $\gamma \rightarrow 0$  and the absorption coefficient becomes proportional to  $E^{1/2}$  or  $E^{3/2}$  for an allowed or a forbidden transition, respectively. A plot of  $\alpha^2$  or  $\alpha^{2/3}$  vs  $h\nu$  will then give a linear behavior from which one can determine  $E_g$ . In neither case did we find a linear behavior, but a better result was obtained for a forbidden transition. From these considerations we conclude that the band gap transition of Cs<sub>3</sub>Bi<sub>2</sub>Cl<sub>9</sub> is a direct forbidden one.

If we have a forbidden transition then the first line of the Wannier series is missing, so the observed line at 3.140 eV is the  $n = 2$  line. In emission a very weak band edge luminescence was observed with a sharp line at 3.132 eV. In our opinion this sharp line is the  $n = 1$  exciton line of the Wannier series which can only be observed in emission at very low temperatures due to the forbidden character of this transition. From the positions of the  $n = 1$  and  $n = 2$  lines the binding energy of the exciton and the band gap can now be calculated:  $G = 11$  meV and  $E_g = 3.143$  eV. The weak line at 3.142 eV in the absorption spectrum is due to the  $n = 3$  line of the Wannier series. The lines observed at 3.145 and 3.152 eV do not belong to this hydrogenic series. They are probably phonon replicas of the  $n = 1$  and  $n = 2$  exciton lines. Both lines are about 12 meV ( $\approx 100$  cm<sup>-1</sup>) higher in energy than the corresponding exciton lines. Since detailed band structure calculations are not available, we will not discuss the forbidden character of the band gap transition further. Finally, we note that the exciton binding

energies which we have found for  $\text{Cs}_3\text{Bi}_2\text{Cl}_9$  (11 meV) and  $\text{Cs}_3\text{Bi}_2\text{Br}_9$  (6 meV) compare well with those observed for the corresponding simple cubic thallos halides (12).

Of the two excitation bands at higher energies the band at about 3.8 eV is probably due to a charge transfer transition from the chlorine 3p band to the bismuth conduction band. This transition takes place at higher energies than the corresponding transition in  $\text{Cs}_3\text{Bi}_2\text{Br}_9$  (~3 eV), since chlorine is more electronegative than bromine. The thallos halides and the cesium lead halides show the same behavior (12, 3).

The excitation band at 3.4 eV undoubtedly corresponds to the emission band at 1.5 eV, since its intensity relative to that of the band edge transition depends on the emission wavelength monitored. Evidently this center can be excited in two ways: directly into the center or by band gap excitation. Since the 3.4-eV excitation band lies above the band gap, we conclude that these centers are concentrated at the surface of our crystals, because exciting radiation with this energy cannot penetrate deeply into the crystal.

As in cesium bismuth bromide, the red luminescence is probably due to bismuth ions coordinated by one or more oxygen ions. Since the edge luminescence is much weaker than the impurity luminescence we conclude that the concentration of these impurities is relatively high. The infrared spectrum of the  $\text{Cs}_3\text{Bi}_2\text{Cl}_9$  crystals shows absorption bands around 3500 and 1600  $\text{cm}^{-1}$ , indicating a certain concentration of hydroxyl ions in the crystals. At about 500  $\text{cm}^{-1}$  another absorption band is observed which can be ascribed to a bismuth-oxygen vibration. Comparable values were found for the totally symmetric  $\text{Bi}^{3+}-\text{O}^{2-}$  stretching vibration in CaO (13) and in  $\text{NaLnO}_2$  ( $\text{Ln} = \text{Sc}, \text{Lu}, \text{Y}, \text{Gd}$ ) (9). The totally symmetric bismuth-chlorine vibration is expected at much lower energies, viz., around 300  $\text{cm}^{-1}$  (14).

Whereas the infrared spectrum shows the presence of oxygen in the red-emitting centers, the temperature dependence of the decay time is strong evidence for a  $\text{Bi}^{3+}$  ion in this center (1, 10). The decay time at low temperatures (~80  $\mu\text{sec}$ ) is relatively short for a pure  ${}^3P_0-{}^1S_0$  transition. On the other hand, at higher temperatures the decay time should be very short ( $\leq 1 \mu\text{sec}$ ) if a pure  ${}^3P_1-{}^1S_0$  transition is involved. Similar behavior was found for other bismuth-containing compounds (15, 16). In all these compounds the bismuth ion is surrounded by three ligands with a short bond length and by three other ones which lie further away from the central ion. The red-emitting center has probably even lower site symmetry due to the presence of the hydroxyl group. This makes a mixing of the  ${}^3P_1$  and  ${}^3P_0$  levels possible, especially because their energy difference is very small (see above). In this way the  ${}^3P_0$  level will have a certain  ${}^3P_1$  character which will lead to a shorter decay time at low temperatures. On the other hand, the  ${}^3P_1$  level will have a little bit of  ${}^3P_0$  character, which will make this transition more forbidden.

The 1.9-eV emission is ascribed to a " $\text{Bi}^{3+}-\text{OH}^-$ " center in the bulk. As argued above, the concentration of this center is higher than in  $\text{Cs}_3\text{Bi}_2\text{Br}_9$ , preventing the occurrence of strong edge emission. This higher concentration can be ascribed to the fact that the difference in size between  $\text{OH}^-$  and  $\text{Cl}^-$  is less than that between  $\text{OH}^-$  and  $\text{Br}^-$ . The surface center may consist of an oxidized layer in or on the surface of the crystal. The 3.05-eV emission is due to bound exciton recombination. A similar observation has been made for  $\text{Cs}_3\text{Bi}_2\text{Br}_9$  (1).

## 2. Luminescence of $\alpha\text{-Cs}_3\text{Sb}_2\text{Cl}_9$

At liquid helium temperature crystals of  $\alpha\text{-Cs}_3\text{Sb}_2\text{Cl}_9$  show a weak, green luminescence. When the temperature is raised to about 20K, the luminescence intensity in-

creases considerably. The emission and excitation spectra of the luminescence of  $\alpha\text{-Cs}_3\text{Sb}_2\text{Cl}_9$  crystals at 4.2K are shown in Fig. 4. The emission spectrum consists of one Gaussian band with a maximum at 2.32 eV. The excitation spectrum of this band is more complex. The spectrum starts on the low-energy side with two lines, viz., at 3.025 and 3.055 eV. These are followed by a strong and narrow excitation band which peaks at 3.09 eV. At still higher energies a broad band is observed with a maximum at about 3.7 eV.

This excitation spectrum is comparable with that of  $\text{Cs}_3\text{Bi}_2\text{Cl}_9$  (Fig. 2). The excitation band at 3.09 eV is due to the band gap transition. By analogy we assume that the upper valence band is formed by  $\text{Sb}^{3+}$  ( $5s$ ) functions and the conduction band by  $\text{Sb}^{3+}$  ( $5p$ ) functions. The band at 3.7 eV is ascribed to a charge transfer transition of the  $\text{Cl}^-$  ( $3p$ ) band to the antimony conduction band. In  $\text{Cs}_3\text{Bi}_2\text{Cl}_9$  the corresponding transitions were observed at 3.20 and 3.8 eV. The sharp lines on the low-energy side of the band edge are transitions to cationic exciton states. Since no edge emission could be observed upon band edge excitation, it is hard to decide on the nature of this exciton. If we take the sharpness of the lines as an indication for a direct transition and their

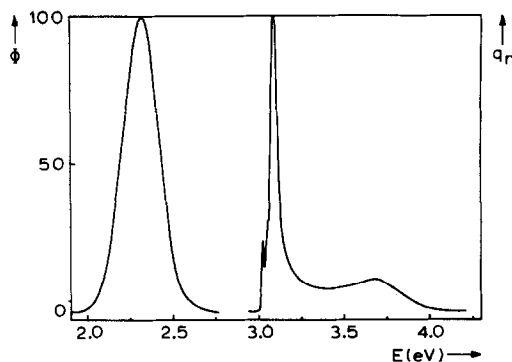


FIG. 4. Emission and excitation spectra of the luminescence of  $\alpha\text{-Cs}_3\text{Sb}_2\text{Cl}_9$  at 4.2K. The emission spectrum was recorded for excitation into the band edge at 3.1 eV.

low intensity as an indication for a forbidden transition, we arrive at the same results as for  $\text{Cs}_3\text{Bi}_2\text{Cl}_9$  and  $\text{Cs}_3\text{Bi}_2\text{Br}_9$  (4), i.e., the band gap transition is direct, but forbidden.

If the two lines belong to the same excitation series, we obtain  $G = 40$  meV and  $E_g = 3.065$  eV if the two lines correspond to  $n = 1$  and  $n = 2$ , and we obtain  $G = 220$  meV and  $E_g = 3.08$  eV if the lines correspond to  $n = 2$  and  $n = 3$  (i.e., when the  $n = 1$  transition is completely forbidden). The latter binding energy seems to be exceptionally large, so we prefer the former set of data.

In  $\text{Cs}_3\text{Bi}_2\text{Cl}_9$  and  $\text{Cs}_3\text{Bi}_2\text{Br}_9$  the emission bands at low energies were ascribed to luminescence from  $\text{Bi}^{3+}$  centers which contain oxygen on halide sites. Since crystals of these compounds were grown from an aqueous solution, it is very likely that oxygen is built into the crystals. The chloride contains more oxygen (probably as  $\text{OH}^-$ ) than the bromide. We conclude that the green luminescence of  $\alpha\text{-Cs}_3\text{Sb}_2\text{Cl}_9$  is also due to  $\text{Sb}^{3+}$  ions which are coordinated by one or more oxygen ions. These centers act as traps for free electrons or holes which are created by excitation into the band gap. In  $\text{Cs}_3\text{Bi}_2\text{Cl}_9$  a weak edge emission could be observed. In  $\alpha\text{-Cs}_3\text{Sb}_2\text{Cl}_9$  no edge luminescence was observed at all. This indicates that there are a large number of impurity centers in this compound.

Results of temperature-dependent measurements on the green emission are presented in Fig. 5. Note that at 4.2K the emission intensity is at a very low level. Above 7K the intensity starts to increase. A maximum is reached at about 18K. Above this temperature the intensity decreases again due to thermal quenching of the luminescence. The decay time is about 370  $\mu\text{sec}$  at liquid helium temperature. Above 8K the decay time decreases rapidly. At 20K it has reached a value of about 20  $\mu\text{sec}$ .

The observed curves can be explained, if we assume a three-level scheme as given in the inset of Fig. 5. Here it should be kept in

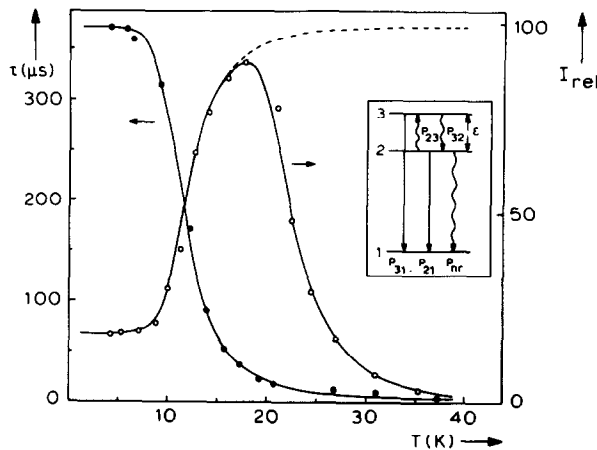


FIG. 5. Emission intensity (O) and decay time (●) of the green luminescence of  $\alpha$ - $\text{Cs}_3\text{Sb}_2\text{Cl}_9$ , as a function of temperature. The three-level scheme (inset) is discussed in the text.

mind that the luminescent center contains a  $\text{Sb}^{3+}$  ion, so the levels 1, 2, and 3 correspond to the levels  $^1S_0$ ,  $^3P_0$ , and  $^3P_1$  of a  $\text{Sb}^{3+}$  ( $5s^2$ ) ion, respectively. Since the radiative  $2 \rightarrow 1$  transition is strongly forbidden, a nonradiative transition probability  $P_{nr}$  has been introduced. This competes with  $P_{21}$ . Since  $P_{31} \gg P_{21}$ , nonradiative transitions from 3 to 1 are neglected in this model. This can only be done at low temperatures.  $P_{23}$  and  $P_{32}$  are nonradiative transition probabilities:  $P_{32} \gg P_{31} \gg P_{21}$ . If we assume a Boltzmann distribution between the population of the levels 2 and 3, then  $P_{23}/P_{32} = \exp(-\epsilon/kT)$ . The thermal quenching above 20K is accounted for by a nonspecified process requiring an activation energy  $\Delta E$ .

For such a scheme the following expressions for the integrated intensity and the decay time have been derived (17):

$$I(T) = \frac{N}{1 + C \exp(-\Delta E/kT)} \cdot \frac{P_{21} + P_{31} \exp(-\epsilon/kT)}{P_{21} + P_{nr} + P_{31} \exp(-\epsilon/kT)},$$

$$\tau(T) = \frac{1 + \exp(-\epsilon/kT)}{P_{21} + P_{nr} + P_{31} \exp(-\epsilon/kT)}.$$

$C$  is a constant related to the nonradiative

transition probability for thermal quenching. For simplicity we have neglected the thermal quenching in the expression for  $\tau$ . This means that the expression is only valid for temperatures below 18K.

The best fit to both curves was obtained with the following data:  $P_{21} = 485 \text{ sec}^{-1}$ ;  $P_{31} = 2.72 \cdot 10^6 \text{ sec}^{-1}$ ;  $P_{nr} = 2210 \text{ sec}^{-1}$ ;  $C = 10400$ ;  $\epsilon = 7 \text{ meV}$  and  $\Delta E = 18 \text{ meV}$ . The dashed line in Fig. 5 gives the estimated curve, if no thermal quenching occurs.

The radiative decay times  $1/P_{21}$  ( $=2.1 \text{ msec}$ ) and  $1/P_{31}$  ( $=0.4 \text{ } \mu\text{sec}$ ) belong to the  $^3P_0 \rightarrow ^1S_0$  and  $^3P_1 \rightarrow ^1S_0$  transitions of the  $\text{Sb}^{3+}$  ion, respectively. These decay times are longer than those for the corresponding transitions of a bismuth ion (10). This is because the weaker spin-orbit coupling of antimony enhances the spin selection rule.

### 3. Luminescence of $\beta$ - $\text{Cs}_3\text{Sb}_2\text{Cl}_9$

At room temperature yellow-colored crystals of  $\beta$ - $\text{Cs}_3\text{Sb}_2\text{Cl}_9$  show absorption at energies higher than 3 eV. These crystals do not luminesce, not even at liquid helium temperature. If the crystals were kept in air for a few days, a very weak, yellow luminescence was observed upon excitation in the uv. This phenomenon was also ob-

served for the  $\alpha\text{-Cs}_3\text{Sb}_2\text{Cl}_9$  crystals, where a yellow emission appeared in addition to the green emission reported above. The yellow emission intensity increased when the crystals were kept for a longer period in air. Simultaneously a white-colored layer was formed on the surface of the crystals. From this we conclude that the yellow luminescence originates from a product formed by reaction of  $\text{Cs}_3\text{Sb}_2\text{Cl}_9$  with air. The surface luminescence consists of one broad emission band with a maximum at 2.2 eV. The half-width of this emission band is about 0.4 eV. The excitation spectrum consists of a band peaking at 3.8 eV and a weaker one peaking at 4.3 eV. The luminescence quenches at temperatures higher than 160K.

At low temperatures the yellow emission has a very long decay time of about 1.5 msec. The decay time decreases very rapidly above 10K. At 25K the decay time has decreased to 15  $\mu\text{sec}$ . Above 100K a constant level of 1.3  $\mu\text{sec}$  is reached until thermal quenching of the luminescence sets in.

Although it is not known what kind of compound is formed on the surface (probably an antimony oxychloride), the observed decay times and their temperature dependence point to luminescence from  $\text{Sb}^{3+}$  ions. At low temperatures the emitting level is  $^3P_0$ ; at higher temperatures the transition is from  $^3P_1$  to  $^1S_0$ . The energy difference derived from the decay time measurements is 7 meV. The results are comparable with those for the luminescence of the defect centers in  $\alpha\text{-Cs}_3\text{Sb}_2\text{Cl}_9$  which are ascribed to antimony positioned next to an oxygen impurity.

According to Ref. (18)  $\text{Cs}_3\text{Sb}_2\text{Cl}_9$  is a white compound at room temperature. At higher temperatures its color changes from white to yellow. This means that the yellow color of our crystals, which is even present at liquid nitrogen temperature, is not intrinsic but is caused by the presence of defects or impurities. There is reason to believe

that our crystals contain a small amount of pentavalent antimony. The mixed-valence compound  $\text{Cs}_2\text{Sb}_{0.5}^{3+}\text{Sb}_{0.5}^{5+}\text{Cl}_6$  shows a very intense color due to the intervalence charge transfer transition of  $\text{Sb}^{3+}$  to  $\text{Sb}^{5+}$  which has a very high absorption strength (19). Dilute solid solutions (concentration less than 5%) are yellow like our crystals. We feel that these pentavalent antimony ions act as killer centers for the luminescence of  $\beta\text{-Cs}_3\text{Sb}_2\text{Cl}_9$  (also see below).

As mentioned above, we succeeded in growing some colorless crystals from solution. X-Ray diffraction shows that these crystals are  $\beta\text{-Cs}_3\text{Sb}_2\text{Cl}_9$ . The absorption spectrum at room temperature consists of two intense broad absorption regions: one around 3.7 eV and one at energies higher than 4.3 eV, at which energy a clear absorption minimum occurs. At 4.2K the crystals show a very intense luminescence in the uv. The emission and excitation spectra are given in Fig. 6. The emission spectrum consists of one band peaking at 3.23 eV. No visible emission is observed. The excitation spectrum of the emission consists of several bands. The main peaks lie between 3.5 and 4.3 eV. This region coincides with the first, broad absorption region. Weaker excitation bands are found above 4.3 eV. The excitation minima in the first absorption re-

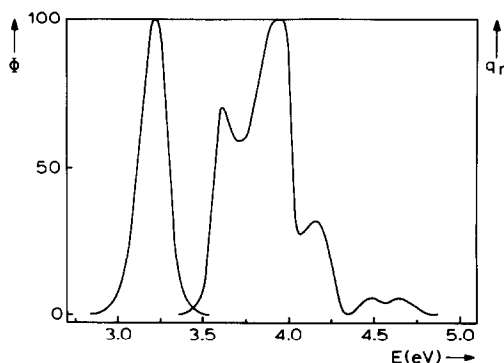


FIG. 6. Emission and excitation spectra of the luminescence of  $\beta\text{-Cs}_3\text{Sb}_2\text{Cl}_9$  at 4.2K. The emission spectrum was recorded for excitation at 3.9 eV.



gion are considered to be maxima in the absorption spectrum. This phenomenon is common for highly concentrated compounds. In this way we conclude that there are two absorption maxima, one at 3.75 eV and another at about 4.1 eV.

The spectra of  $\beta\text{-Cs}_3\text{Sb}_2\text{Cl}_9$  look different from those of the other halides under consideration. First, the excitation spectrum shows no exciton absorption lines and no band gap-like transition. Second, we observe uv emission and no trap emission from deep defect centers, whereas we did observe trap emission in the other halides. Therefore we assume that we are dealing with transitions localized on the  $\text{Sb}^{3+}$  ions. By comparison with the transitions in the compound  $\text{MgS-Sb}^{3+}$ , which lie roughly in the same spectral region (20), we arrive at the following assignments: the absorption peak at 3.7 eV is due to the  $^1S_0\text{-}^3P_1$  transition, and the one at about 4.6 eV to the  $^1S_0\text{-}^1P_1$  transition. The band near 4.1 eV may be assigned to  $^1S_0\text{-}^3P_2$ . The emission is due to the  $^3P_{1,0}\text{-}^1S_0$  transition.

It is now obvious why the yellow-colored crystals do not luminesce. The luminescence of pure  $\beta\text{-Cs}_3\text{Sb}_2\text{Cl}_9$  crystals peaks at 3.23 eV. This is in the region where the yellow-colored crystals show very strong absorption due to the intervalence charge transfer. Because of this excellent spectral overlap and the high oscillator strength of the intervalence charge transfer transition, energy transfer can take place with high efficiency and over long distances. Charge transfer states show considerable relaxation, which makes nonradiative return to the ground state likely. Krol *et al.* (21) have explained the absence of luminescence in certain  $\text{U}^{6+}$  compounds in exactly the same way as we have done for a  $\text{Sb}^{3+}$  compound.

Below 40K the decay time of the emission has a value of about 470  $\mu\text{sec}$  (see Fig. 7). Above 40K the decay time decreases steeply. This decrease coincides with the quenching range in the luminescence inten-

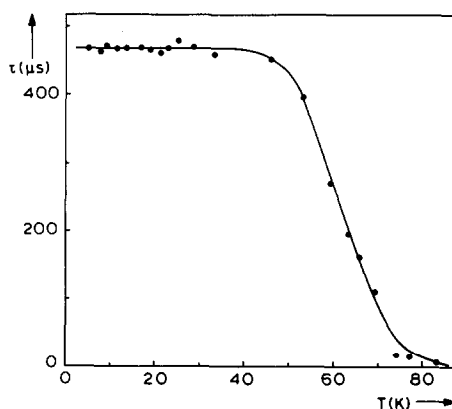


FIG. 7. Decay time of the uv emission of  $\beta\text{-Cs}_3\text{Sb}_2\text{Cl}_9$  as a function of temperature.

sity vs temperature curve. By comparison with standard phosphors the quantum efficiency of the uv emission at low temperature is estimated to be 30%. This yields a radiative decay time of about 1.5 msec, which is in good agreement with values mentioned above.

In view of the Stokes shift and the absence of purely electronic lines in the spectra, energy migration among the  $\text{Sb}^{3+}$  ions can be ruled out at liquid helium temperature (22). The relatively low quantum efficiency may be due to one-step energy transfer to  $\text{Sb}^{5+}$  killer sites, which may also be present in colorless crystals. The absorption spectrum in fact shows a very weak tail in the charge transfer area. Although the concentration of these ions must be very low, energy transfer is very effective (see above).

There are two possible mechanisms which may be involved in the thermal quenching above 40K: (a) thermal quenching in the same  $\text{Sb}^{3+}$  ion as the one in which the excitation takes place (this does not seem probable in view of the relatively small Stokes shift) (20, 23); and (b) energy migration among the  $\text{Sb}^{3+}$  sublattice followed by nonradiative decay at killer sites. This seems to be a more probable mechanism. The killer sites might be  $\text{Sb}^{3+}$  ions

positioned next to oxygen (which are quenched above 40K, see above) or  $\text{Sb}^{5+}$  ions.

Kellendonk *et al.* explained the observed energy migration in bismuth aluminum borate at low temperatures in terms of energy migration via the  $^3P_1$  level (24). They found that the transfer probability ( $\sim 10^{10} \text{ sec}^{-1}$ ) is larger than the nonradiative decay rate from  $^3P_1$  to  $^3P_0$  ( $P_{32} \approx 10^9 \text{ sec}^{-1}$ ). In  $\beta\text{-Cs}_3\text{Sb}_2\text{Cl}_9$ , energy migration among the antimony sublattice occurs only at higher temperatures, i.e., when the  $^3P_1$  level becomes thermally occupied. This means that the transfer probability is less than  $P_{32}$ , but larger than the radiative transition probability of the  $^3P_1 \rightarrow ^1S_0$  transition ( $P_{31} = 10^6 \text{ sec}^{-1}$ ). The  $\text{Sb}^{3+}\text{-Sb}^{3+}$  distance in our compound is shorter than the  $\text{Bi}^{3+}\text{-Bi}^{3+}$  distance in  $\text{Y}_{0.77}\text{Bi}_{0.23}\text{Al}_3\text{B}_4\text{O}_{12}$ , but the spectral overlap and the absorption strength are smaller. Therefore a transfer probability of  $10^7 \text{ sec}^{-1}$  seems reasonable. This means that below 40K the excited  $\text{Sb}^{3+}$  ion relaxes to the  $^3P_0$  level, from which emission occurs. Above 40K energy migration among the  $\text{Sb}^{3+}$  ions occurs via the  $^3P_1$  level until the migrating energy is trapped by killer sites. The luminescence of  $\beta\text{-Cs}_3\text{Sb}_2\text{Cl}_9$  is concentration quenched above 40K.

The observed energy difference of about 50 meV between  $^3P_1$  and  $^3P_0$  seems to be a rather large value for  $\text{Sb}^{3+}$  in view of the weak spin-orbit splitting compared to the bismuth ion. However, there is a lack of accurate data in literature, so no comparisons are possible.

#### 4. Influence of the Structure

Of the compounds investigated, viz.,  $\text{Cs}_3\text{Bi}_2\text{Br}_9$ ,  $\text{Cs}_3\text{Bi}_2\text{Cl}_9$ ,  $\alpha\text{-}$  and  $\beta\text{-Cs}_3\text{Sb}_2\text{Cl}_9$ , the first three show optical transitions, which must be described with a band model. Crystals of  $\beta\text{-Cs}_3\text{Sb}_2\text{Cl}_9$ , on the other hand, show transitions which are localized on the  $\text{Sb}^{3+}$  ion. Obviously, slight structural changes are able to induce the transition

from localized to delocalized. The compounds  $\text{Cs}_3\text{Bi}_2\text{Br}_9$  and  $\alpha\text{-Cs}_3\text{Sb}_2\text{Cl}_9$  have almost the same crystal structure and show comparable luminescence properties. Even the exciton spectra are similar. The compounds  $\text{Cs}_3\text{Bi}_2\text{Cl}_9$  and  $\beta\text{-Cs}_3\text{Sb}_2\text{Cl}_9$  are also isomorphous with a different crystal structure from that of  $\text{Cs}_3\text{Bi}_2\text{Br}_9$  and  $\alpha\text{-Cs}_3\text{Sb}_2\text{Cl}_9$ . Cesium bismuth chloride still shows delocalized behavior with a more strongly forbidden  $n = 1$  exciton transition, while  $\beta\text{-Cs}_3\text{Sb}_2\text{Cl}_9$  shows localized  $\text{Sb}^{3+}$  transitions.

In Fig. 8 the relevant part of both structures is drawn. From this picture it is clear that the two structures do not only differ in stacking sequence, as discussed in the introduction of this paper, but there is also a great difference in the orientation of the lone-pair lobes of the  $ns^2$  ions. The so-called lone pair effect causes the lengthening of the metal-halogen bonds due to the repulsive forces between the lone pair and the negatively charged halogen ion. In such a configuration the lone pair will point in the direction of the center of mass of the three more distant halogen ions (25). In the structure of  $\text{Cs}_3\text{Bi}_2\text{Br}_9$  and  $\alpha\text{-Cs}_3\text{Sb}_2\text{Cl}_9$  this results in a parallel orientation of the lone pair lobes (see Fig. 8a). The lobes point to-

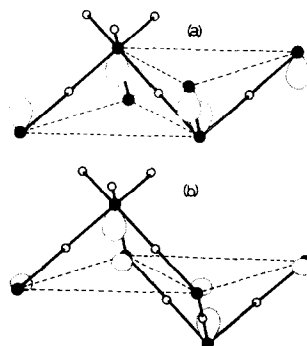


FIG. 8. Part of the structures of  $\text{Cs}_3\text{Bi}_2\text{Br}_9$  and  $\alpha\text{-Cs}_3\text{Sb}_2\text{Cl}_9$  (a) and  $\text{Cs}_3\text{Bi}_2\text{Cl}_9$  and  $\beta\text{-Cs}_3\text{Sb}_2\text{Cl}_9$  (b). Black spheres represent  $ns^2$  ions and white spheres halide ions. The orientations of the  $ns^2$  lone pair orbitals are shown schematically.

ward the inside of the double layer. This makes an effective overlap between the lone pair lobes possible.

The overlap between the lone pair orbitals of the compounds  $\text{Cs}_3\text{Bi}_2\text{Cl}_9$  and  $\beta\text{-Cs}_3\text{Sb}_2\text{Cl}_9$  is smaller, as can be seen from Fig. 8b. Here the lobes are perpendicular to each other. Since overlap between the  $ns^2$  orbitals is required for the formation of the cationic valence band, it is concluded that compounds with the  $\alpha$  structure will show a stronger tendency to delocalization than compounds with the  $\beta$  structure.

Nevertheless,  $\text{Cs}_3\text{Bi}_2\text{Cl}_9$  also shows delocalized optical properties. This may be due to the fact that the  $6s^2$  lone pair of  $\text{Bi}^{3+}$  has a larger extension than the  $5s^2$  lone pair of antimony. Another possible explanation is that the bismuth-chlorine octahedra in  $\text{Cs}_3\text{Bi}_2\text{Cl}_9$  (l.t.) are strongly distorted (see Table I). One of the longer-bonded chlorine ions is positioned closer to one bismuth ion than to the other which results in a short (2.60 Å) and a very long bond length (3.08 Å). In this configuration the lone pair lobe of the first bismuth ion will move slightly away from the shorter-bonded chlorine ion, while the lone pair lobe of the second bismuth ion will orient itself along the longer bond. This will result in a more parallel orientation of the lone pair lobes, which consequently may increase the size of the overlap. Obviously, band structure calculations are necessary to confirm these speculative considerations.

Recently the luminescence properties of  $\text{CsSnBr}_3$  have been reported in the literature (26). This compound shows semiconductor behavior with  $E_g = 1.8$  eV (compare  $\text{CsPbBr}_3 \sim 2.4$  eV (3)). Both edge emission (1.7–1.8 eV) and deep-center emission (1.16 eV) were reported. The present results tempt one to give an interpretation that differs from that given by the authors of Ref. (26). The edge emission is due to recombination of cationic bound excitons, and the deep-center emission is due to a

$\text{Sn}^{2+}-\text{O}^{2-}$  complex. The thermal quenching temperature of the edge emission in  $\text{CsSnBr}_3$  is considerably higher than in our compounds. The  $\text{CsSnBr}_3$  was not prepared from an aqueous solution. It cannot be ruled out that our preparation procedure induces certain killer sites which are responsible for the low quenching temperatures. The high  $\text{OH}^-$  vibrational frequency might play an important role in this quenching process.

### Acknowledgments

The investigations were carried out as part of the research program of the Stichting voor Fundamenteel Onderzoek der Materie (FOM) and with financial support from the Nederlandse Organisatie voor Zuiver Wetenschappelijk Onderzoek (ZWO).

### References

1. C. W. M. TIMMERMANS AND G. BLASSE, *Phys. Status Solidi B* **106**, 647 (1981).
2. K. HEIDRICH, H. KÜNZEL, AND J. TREUSCH, *Solid State Commun.* **25**, 887 (1978).
3. K. HEIDRICH, W. SCHÄFER, M. SCHREIBER, J. SÖCHTIG, G. TRENDEL, J. TREUSCH, T. GRANDKE, AND H. J. STOLZ, *Phys. Rev. B* **24**, 5642 (1981).
4. C. W. M. TIMMERMANS, S. O. CHOLAKH, AND G. BLASSE, *Phys. Status Solidi B* **115** (1983).
5. G. MEIJER AND A. SCHÖNEMUND, *Z. Anorg. Allg. Chem.* **468**, 185 (1980).
6. F. LAZARINI, *Acta Crystallogr. B* **33**, 2961 (1977).
7. K. KIHARA AND T. SUDO, *Acta Crystallogr. B* **30**, 1088 (1974).
8. K. KIHARA AND T. SUDO, *Z. Kristallogr.* **134**, 142 (1971).
9. A. C. VAN DER STEEN, J. J. A. VAN HESTEREN, AND A. P. SLOK, *J. Electrochem. Soc.* **128**, 1327 (1980).
10. G. BOULON, *J. Phys.* **32**, 333 (1971).
11. R. J. ELLIOTT, *Phys. Rev.* **108**, 1384 (1957).
12. R. Z. BACHRACH AND F. C. BROWN, *Phys. Rev. B* **1**, 818 (1970).
13. A. E. HUGHES AND G. P. PELS, *Phys. Status Solidi B* **71**, 707 (1975).
14. A. C. VAN DER STEEN, *Phys. Status Solidi B* **100**, 603 (1980).
15. C. W. M. TIMMERMANS, O. BOEN HO, AND G. BLASSE, *Solid State Commun.* **42**, 505 (1982).

16. G. Blasse and O. Boen Ho, *J. Lumin.* **21**, 165 (1980).
17. W. VAN LOO, *J. Lumin.* **10**, 221 (1975).
18. S. J. CLARK, J. D. DONALDSON, AND D. R. LAUGHLIN, *J. Solid State Chem.* **41**, 143 (1982).
19. P. DAY, *Inorg. Chem.* **2**, 452 (1963).
20. S. ASANO AND N. YAMASHITA, *J. Phys. Soc. Japan* **49**, 2231 (1980).
21. D. J. KROL, J. P. M. ROS, AND A. ROOS, *J. Chem. Phys.* **73**, 1521 (1980).
22. R. C. POWELL AND G. BLASSE, *Struct. Bonding* **42**, 43 (1980).
23. G. BLASSE AND G. J. DIRKSEN, *Phys. Status Solidi B* **110**, 487 (1982).
24. F. KELLENDONK, T. VAN DEN BELT, AND G. BLASSE, *J. Chem. Phys.* **76**, 1194 (1982).
25. J. GALY, G. MEUNIER, S. ANDERSSON, AND A. ÅSTRÖM, *J. Solid State Chem.* **13**, 142 (1975).
26. S. J. CLARK, C. D. FLINT, AND J. D. DONALDSON, *J. Phys. Chem. Solids* **42**, 133 (1981).